Ultrasonics 53 (2013) 849–852

Contents lists available at SciVerse ScienceDirect

Ultrasonics

journal homepage: www.elsevier.com/locate/ultras

The slow zero order antisymmetric Lamb mode in phononic crystal plates

Jun Liu [a,b], Feng Li [a], Yihui Wu [a,*]

[a] State Key Laboratory of Applied Optics Changchun Institute of Optics, Fine Mechanics and Physics, Chinese Academy of Sciences, Changchun 130033, China
[b] Graduate University of Chinese Academy of Sciences, Beijing 100039, China

ARTICLE INFO

Article history:
Received 10 August 2012
Received in revised form 4 December 2012
Accepted 5 December 2012
Available online 12 December 2012

Keywords:
Slow modes
Lamb waves
Phononic crystal plates

ABSTRACT

In this paper, the group velocities of the zero order antisymmetric (A0) Lamb modes in a phononic crystal plate with single layer cylindrical holes parallel to the surface of the plate were investigated theoretically. The results show that by increasing the filling fraction, the A0 mode can be efficiently slowed down and the group velocity of the A0 modes can be tuned from the positive to the negative referring to the phase velocity. Moreover, the zero group velocity of the A0 modes can be obtained with a given filling fraction. These results may be useful in designing acoustic devices.

1. Introduction

In the past decades, slow light effects have been widely studied in the photonic crystals [1–6]. Due to the enhancement of the light-matter interactions, slow light effects can be used for the enhancement of nonlinear effects, light localization, light emission and biosensors. Recently, the slow acoustic wave modes in phononic crystals (PCs) have also attracted much attention [7–15]. It has been shown that, the slow waves can be realized in the waveguides of the phononic crystals and the phoxonic crystals. And the slow surface waves have been verified in the phononic surface. In addition, the slow resonant modes due to the locally resonant effect in the phononic plate with periodic membranes have also been reported.

The zero order antisymmetric (A0) Lamb mode can be applied in liquid environmental sensing thanks to non-leaky evanescent waves in fluid [16]. In order to enhance the resonance and reduce the energy radiating into the substrates for the Lamb wave resonators, the reflective gratings need to be designed, such as the metal strips and phononic crystals [17–21]. Recently, the zero-group-velocity (ZGV) first symmetric Lamb mode (S1) has been applied to the resonators, which can be used as highly sensitive gravimetric sensors without reflective gratings because of the energy localization [22]. In this regard, the ZGV A0 mode could be a good candidate for improving the performance of the Lamb wave resonators for liquid sensing without reflectors. However, this kind of mode could be hardly realized for a homogeneous plate [23]. Motivated from the slow waves in periodic structures, it is hoped that the slow A0 Lamb mode could be obtained by introducing the PCs into the plate.

In this paper, the group velocity of the A0 mode in a plate with single layer cylindrical holes parallel to the surface of the plate were investigated theoretically by changing the filling fractions of the plate. Although the similar structures have been studied, the group velocity of the A0 mode has not been studied up to now, to our knowledge [24–27]. The results show that the A0 mode can be efficiently slowed down by increasing the filling fractions. Moreover, the group velocity of the A0 modes can be tuned from the positive to the negative referring to the phase velocity. Consequently, the ZGV of the A0 mode can be obtained with a given filling fraction. These provide efficient means to manipulate the Lamb wave velocity, enabling the design of acoustic devices, such as delay lines, filters, resonators and biosensors.

2. Models

The three-dimensional profile of the PC plate is shown in Fig. 1a, and a is the lattice constant of the unit cell, h is the thickness of the plate, d is the diameter of the vacuum circle hole, r is the radius. The filling fraction is defined as $f = \pi r^2/(ah)$. Fig. 1b shows the boundary conditions for computing the band structures. The up and down boundaries are set free and the left and right boundaries are set as periodic boundaries. Finite element method which is proved to be an efficient method is used to compute the band structures [28]. For simplification, the parameters of the material is chosen as Young's module $E = 131$ GPa, Poisson's ratio $v = 0.27$, density $\rho = 2330$ kg/m^3 and dissipation is neglected.

* Corresponding author. Tel.: +86 043186176915; fax: +86 043185690271.
E-mail address: yihuiwu@ciomp.ac.cn (Y. Wu).

0041-624X/$ - see front matter © 2012 Elsevier B.V. All rights reserved.
http://dx.doi.org/10.1016/j.ultras.2012.12.005

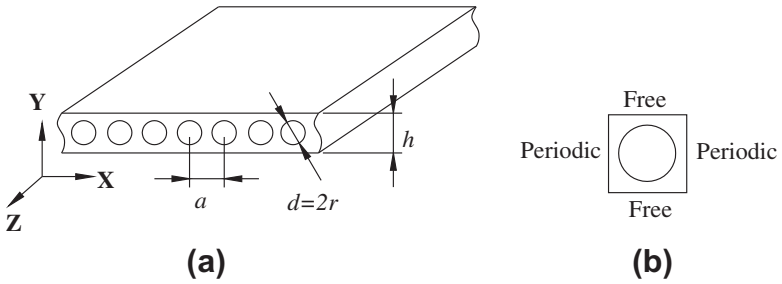

Fig. 1. The model investigated in this paper: (a) the three-dimensional profile of the phononic crystal plate and (b) the boundary conditions imposed on the boundary of the unit cell: the up and down boundaries are set free and the left and right boundaries are set as periodic boundaries.

3. Numerical results and discussions

The band structures for $a = 3$ mm, $h = 0.21$ mm, i.e. $h/a = 0.07$ are shown in Fig. 2a with the radius $r = 0.1$ mm. In the frequency range from 0 to 3 MHz, there are seven branches of the antisymmetric Lamb mode indicated by the solid lines. For simplification, the 1st, 4th and 7th branch were investigated. The displacement components of the 4th and 7th branch at $r = 0.1$ mm and $k_x = 0$ were shown in Fig. 3. It can be seen that, the displacements of both branches in the x direction are antisymmetric with the mid plane and the displacements in the y direction are symmetric with the mid plane. In addition, the modal distributions match well with the modal of the A0 Lamb mode. Thus, both the 4th and 7th branch are A0 mode.

In order to investigate the slowing of the A0 mode, the band width of the 1st, 4th and 7th branch of the A0 mode were calculated with the radius increasing as shown in Fig. 2b [13]. Firstly, it can be noted that, as the radius increasing, the band width of both the 4th and 7th branch decreases until a critical value of the radius and then increase. But this is not the case for the first

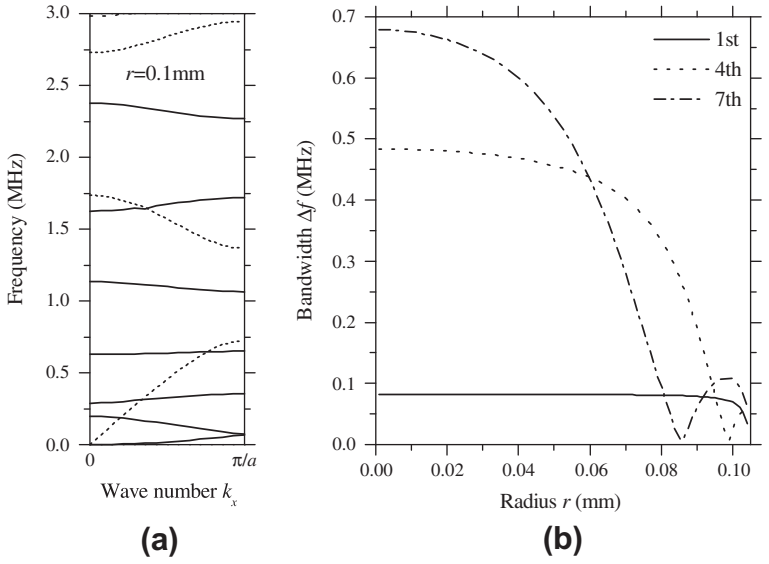

Fig. 2. (a) The band structure when $r = 0.1$ mm, the dotted lines are the branches of the S0 mode and the solid lines are the branches of the A0 mode; (b) the band width of the first, fourth and seventh branch of the A0 mode with the increase of the radius r from 0 to 0.105 mm.

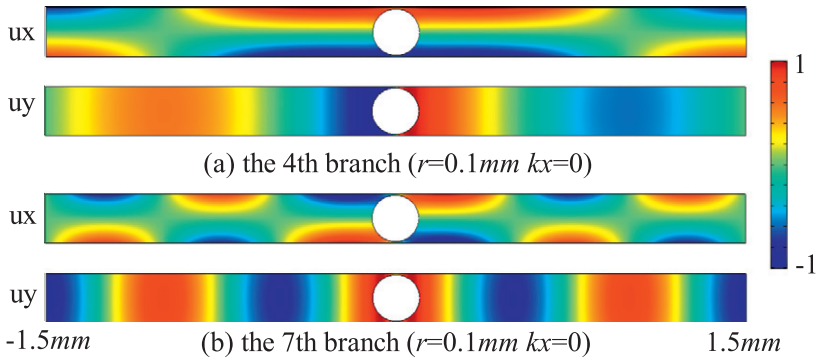

Fig. 3. The displacement components of the (a) 4th branch and (b) 7th branch at $r = 0.1$ mm and $k_x = 0$.

branch. Secondly, it is also shown that, the band width of the branches in high frequency change more significantly than those of the lower branches. As shown, the band width of the 7th branch can be changed from 0.68 MHz to nearly 0 Hz; the bandwidth of the 4th branch is changed from 0.48 MHz to 0 Hz; however the band width of the 1st branch is changed only from 81.7 kHz to 34.8 kHz. For a better understanding, the normalized displacement distributions of the three branches were plotted on the Fig. 4 for $r = 0.1$ mm and $k_x = 0$. It can be seen that, the wavelength λ of the lower branch is longer than the higher branch, as a result, the frequencies of the higher branch can be more sensitive to the change of the radius, when the local stiffness between the cylinder edge and the plate surface becomes weaker as the radius increasing.

For a better understanding of the group velocity of the A0 mode, firstly, the dispersion curves of the 7th branch for radius changing from 0.08 mm to 0.09 mm were depicted in Fig. 5a. It can be seen that, the frequencies at the large wave numbers decrease more significantly than those at the small wave numbers as the radius increasing. This can be explained by the modal distributions for the different wave numbers as shown in Fig. 5b. As shown, the vibration is getting more localized as the increase of the wave number. Thus, the frequencies at the large wave numbers are more sensitive to the increase of the radius than those at the small wave numbers. Then, the group velocity ($\partial\omega/\partial k$) of the 7th branch for $k_x = 0$, $\pi/(4a)$, $\pi/(2a)$, $3\pi/(4a)$ and π/a, with the radius increasing from 0.08 mm to 0.09 mm was calculated as shown in Fig. 6. It

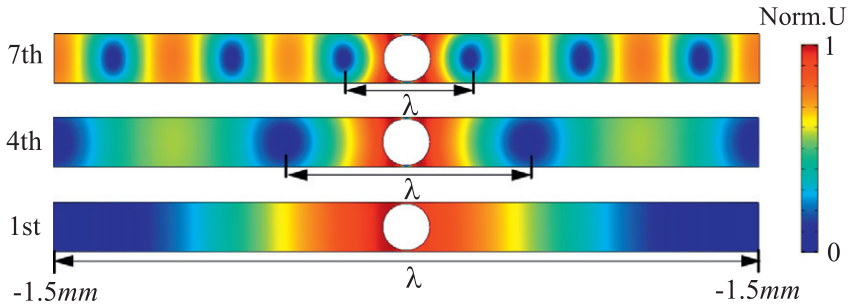

Fig. 4. The modal distributions of the 1st, 4th and 7th branch for $r = 0.1$ mm and $k_x = 0$. The wavelength λ of the lower branch is longer than the higher branch.

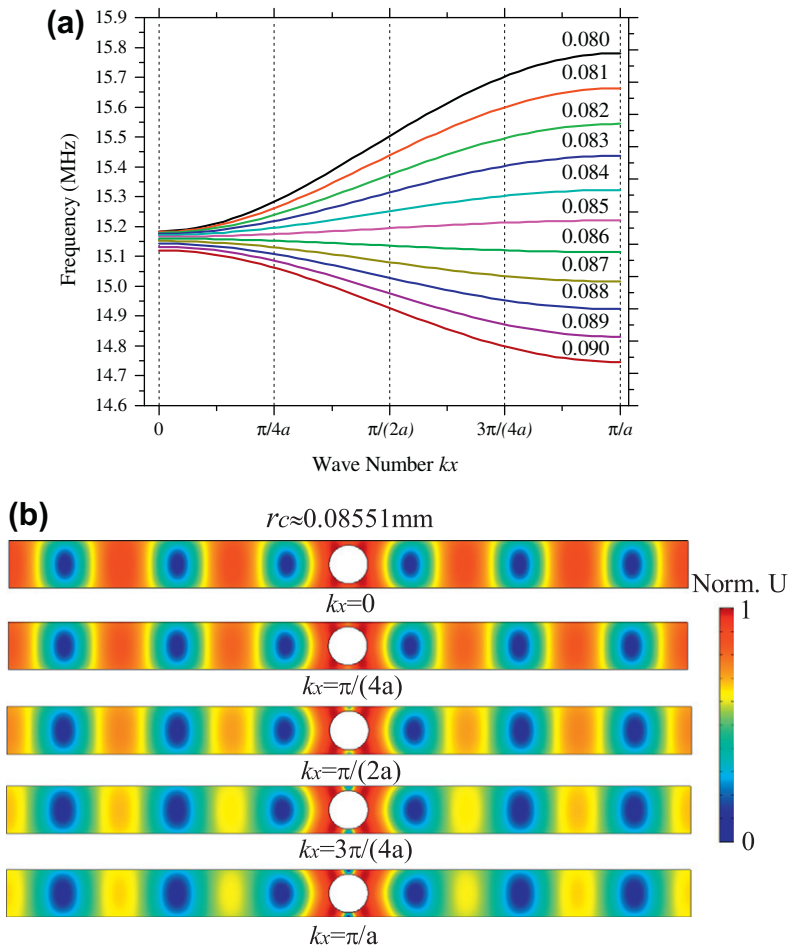

Fig. 5. (a) The dispersion curves of the 7th branch for radius changing from 0.08 mm to 0.09 mm and (b) the modal distributions of the 7th branch when $r = 0.08551$ mm for $k_x = 0$, $\pi/(4a)$, $\pi/(2a)$, $3\pi/(4a)$ and π/a.

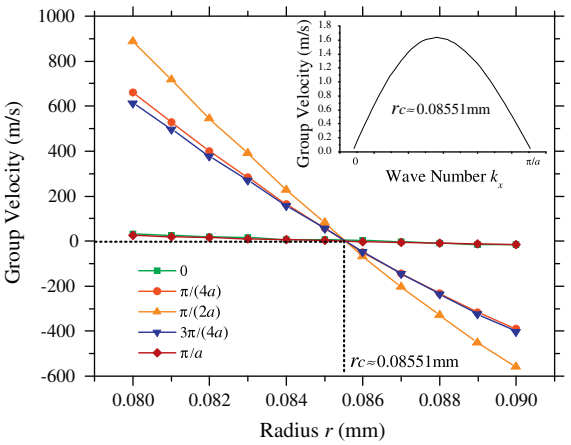

Fig. 6. The group velocity of the seventh branch of the A0 mode when $k_x = 0$, $\pi/(4a)$, $\pi/(2a)$, $3\pi/(4a)$ and π/a, with the radius increasing from 0.08 mm to 0.09 mm; the inset indicates the group velocity of the seventh branch of the A0 mode changes with the wave number as $r = 0.08551$ mm.

can be noted that, for the different wave numbers, the group velocities vary differently with the radius. As shown, when the wave number is at the boundary of the Brillouin zone ($k_x = 0$ or π/a) the group velocities change only in the range about from 30.7 m/s to −14.5 m/s. However when the wave number is in the middle of the Brillouin zone, the group velocities change from 885 m/s to −559 m/s, which demonstrates that the group velocity in the middle of the Brillouin zone can be changed more significantly than that at the boundary of the Brillouin zone. These can also be noted in Fig. 5a, as shown that the slope of the dispersion curves in the middle of the Brillouin zone changes more significantly than that at the boundary of the Brillouin zone.

From Fig. 6, it is also shown that, for all the wave numbers, the group velocities can be tuned from the positive to the negative as the radius increasing and the same critical value of the radius r_c exists for which the group velocities are zero. Through precisely calculation, the r_c exists between 0.08551 mm and 0.08552 mm for the 7th branch. The group velocities when $r = 0.08551$ mm are shown in the inset of Fig. 6. It is shown that, the maximum group velocity with $r = 0.08551$ mm is 1.63 m/s and the band is nearly flat. Thus, it can be concluded that the ZGV A0 mode can be obtained at a filling fraction.

4. Conclusion

In summary, the group velocity of the zero order Lamb modes (A0) of the phononic crystal plate with single layer cylindrical holes parallel to the surface of the plate were investigated theoretically. It is shown that, by increasing the radius or the filling fractions, (a) the A0 mode can be efficiently slowed, (b) the group velocity of the A0 mode can be changed from the positive to the negative and (c) the zero group velocity of the A0 mode can be obtained. These results may be useful in designing acoustic devices, such as delay lines, filters, resonators, biosensors and so on for which the A0 mode is used.

Acknowledgements

The work was funded by the Natural Science Foundation of China (60871043, 60971025 & 11034007), the National High Technology Research and Development Program of China (Grant No. 2012AA040503) and Key Knowledge Innovation Project of The Chinese Academy of Sciences (KJCX2-YW-H18).

References

[1] M. Soljacic, S.G. Johnson, S. Fan, M. Ibanescu, E. Ippen, J.D. Joannopoulos, Photonic-crystal slow-light enhancement of nonlinear phase sensitivity, J. Opt. Soc. Am. B 19 (2002) 2052–2059.
[2] P. Lalanne, J.P. Hugonin, Very large spontaneous-emission β factors in photonic-crystal waveguides, Phys. Rev. Lett. 99 (2007) 023902.
[3] T. Baba, Slow light in photonic crystals, Nat. Photonics 2 (2008) 465–473.
[4] T.F. Krauss, Why do we need slow light?, Nat Photonics 2 (2008) 448–450.
[5] L. Sapienza, H. Thyrrestrup, S. Stobbe, P.D. Garcia, S. Smolka, P. Lodahl, Cavity quantum electrodynamics with anderson-localized modes, Science 327 (2010) 1352–1355.
[6] F. Hosseinibalam, S. Hassanzadeh, A. Ebnali-Heidari, C. Karnutsch, Design of an optofluidic biosensor using the slow-light effect in photonic crystal structures, Appl. Optics. 51 (2012) 568–576.
[7] J. Christensen, P. Huidobro, L. Martín-Moreno, F. García-Vidal, Confining and slowing airborne sound with a corrugated metawire, Appl. Phys. Lett. 93 (2008) 083502.
[8] M.B. Dühring, V. Laude, A. Khelif, Energy storage and dispersion of surface acoustic waves trapped in a periodic array of mechanical resonators, J. Appl. Phys. 105 (2009) 093504.
[9] I. Malfanti, A. Taschin, P. Bartolini, R. Torre, Evidence of slow acoustic surface waves on a 1D phononic surface by a pulsed laser spectroscopic technique resolved in time and space, Europhys. Lett. 97 (2012) 44010.
[10] C.Y. Sun, J.C. Hsu, T.T. Wu, Resonant slow modes in phononic crystal plates with periodic membranes, Appl. Phys. Lett. 97 (2010) 031902.
[11] V. Laude, J.C. Beugnot, S. Benchabane, Y. Pennec, B. Djafari-Rouhani, N. Papanikolaou, J.M. Escalante, A. Martinez, Simultaneous guidance of slow photons and slow acoustic phonons in silicon phoxonic crystal slabs, Opt. Express 19 (2011) 9690–9698.
[12] W.M. Robertson, C. Baker, C.B. Bennett, Slow group velocity propagation of sound via defect coupling in a one-dimensional acoustic band gap array, Am. J. Phys. 72 (2004) 255.
[13] A. Cicek, O. Adem Kaya, M. Yilmaz, B. Ulug, Slow sound propagation in a sonic crystal linear waveguide, J. Appl. Phys. 111 (2012) 013522.
[14] V. Laude, L. Robert, W. Daniau, A. Khelif, S. Ballandras, Surface acoustic wave trapping in a periodic array of mechanical resonators, Appl. Phys. Lett. 89 (2006) 083515.
[15] A. Maznev, A. Every, Surface acoustic waves with negative group velocity in a thin film structure on silicon, Appl. Phys. Lett. 95 (2009) 011903.
[16] D.S. Ballantine, R.M. White, S.J. Martin, A.J. Ricco, E.T. Zellers, G.C. Frye, H. Wohltjen, Acoustic Wave Sensors: Theory, Design, and Physico-Chemical Applications, Academic Press, San Diego, 1997.
[17] D.M. Martin, V. Yantchev, I. Katardjiev, Buried electrode electroacoustic technology for the fabrication of thin film based resonant components, J. Micromech. Microeng. 16 (2006) 1869–1874.
[18] J. Bjurström, I. Katardjiev, V. Yantcheva, Lateral-field-excited thin-film Lamb wave resonator, Appl. Phys. Lett. 86 (2005) 154103.
[19] M. Kadota, T. Ogami, K. Yamamoto, H. Tochishita, $LiNbO_3$ thin film for A1 mode of Lamb wave resonators, Phys. Status Solidi A 208 (2011) 1068–1071.
[20] C.Y. Huang, J.H. Sun, T.T. Wu, A two-port ZnO/silicon Lamb wave resonator using phononic crystals, Appl. Phys. Lett. 97 (2010) 031913.
[21] T.T. Wu, W.S. Wang, J.H. Sun, J.C. Hsu, Y.Y. Chen, Utilization of phononic-crystal reflective gratings in a layered surface acoustic wave device, Appl. Phys. Lett. 94 (2009) 101913.
[22] V. Yantchev, L. Arapan, I. Katardjiev, V. Plessky, Thin-film zero-group-velocity Lamb wave resonator, Appl. Phys. Lett. 99 (2011) 033505.
[23] C. Prada, D. Clorennec, D. Royer, Local vibration of an elastic plate and zero-group velocity Lamb modes, J. Acoust. Soc. Am. 124 (2008) 203–212.
[24] J. Chen, Y. Xia, X. Han, H. Zhang, Lamb waves in phononic crystal slabs: truncated plane parallels to the axis of periodicity, Ultrasonics 52 (2012) 920–924.
[25] J.-J. Chen, H.L.W. Chan, J.-C. Cheng, Large one-dimensional band gaps in three-component phononic crystals plates, Phys. Lett. A 366 (2007) 493–496.
[26] J.-J. Chen, X. Han, The propagation of Lamb waves in one-dimensional phononic crystal plates bordered with symmetric uniform layers, Phys. Lett. A 374 (2010) 3243–3246.
[27] J.-J. Chen, K.-W. Zhang, J. Gao, J.-C. Cheng, Stopbands for lower-order Lamb waves in one-dimensional composite thin plates, Phys. Rev. B 73 (2006) 094307.
[28] A. Khelif, B. Aoubiza, S. Mohammadi, A. Adibi, V. Laude, Complete band gaps in two-dimensional phononic crystal slabs, Phys. Rev. E 74 (2006) 046610.